Specific Chemical Interaction Affecting the Stability of Dispersed Systems

W. Stumm, C. P. Huang, and S. R. Jenkins

*Laboratory of Applied Chemistry, Harvard University,
Cambridge, Massachusetts, 02138, U.S.A.*

1) Sorbable species may destabilize colloids at much lower concentrations than nonsorbable ions. The VODL double layer model neglects the dominating role that chemical forces play in causing adsorption and is restricted in its application to lyophilic colloids and simple electrolytes.

2) The distribution of ions in an oxide-electrolyte interface can be evaluated from alkalimetric and acidimetric titration curves of aqueous dispersions of these oxides.

3) A comparison of the differential capacity of the interface at an oxide-electrolyte interface with that of Hg or AgI shows much larger capacitance values for the hydrophilic strongly aquated oxide surface than for the more hydrophobic surface of Hg and AgI. The difference is caused primarily by the strongly structured, extensively hydrogen-bonded and chemisorbed water layer immediately adjacent to the solid oxide surface. Ions tend strongly to penetrate (specific sorption) into the compact part of the double layer adjoining the oxide surface, and may thus exert a marked effect on the surface chemical properties beyond those observed by a mere compaction of the diffuse part of the double layer.

4) Association of oxide surfaces with H^+, and other cations can, similar as with polyelectrolytes, be characterized by acidity and stability constants. The latter constants can be expressed as intrinsic constants if they are corrected to a hypothetically chargeless surface. The specificity of the interaction with H^+ and cations can be understood by considering simple electrostatic models. This association of oxide surfaces with cations can be used to explain the effect of cations such as Ca^{2+} on the stability of hydrous oxide colloids, and on the deposition of MnO_2 particles on sand surfaces.

The extent to which a coagulant species is specifically adsorbed is reflected in the c. c. c. necessary to produce aggregation. When the specifically adsorbed species and the colloid are of opposite charge, the sorbed species act to reduce the surface charge of the colloid. The destabilizing agent can, in some cases, even reverse the colloid charge and restabilization will occur.

5) Specific cation interactions as described here represent a basis of related ion specific processes, such as the behavior of ion selective glass or membrane electrodes; the selective ion permeability of cell membranes and potential generating mechanisms in the living cell.

Colloid stability is affected by colloid-solvent, coagulant-solvent and colloid-coagulant interactions. The basic theory of the electric double layer (DLVO theory), although a most effective tool in the interpretation of inter-

facial phenomena, describes only one type of coagulant-colloid interaction. Purely chemical factors must be considered in addition to the theory of the double layer in order to explain many of the phenomena pertinent for solid-solution interfaces occurring in natural systems.

This presentation is organized along the following lines: we first discuss in a rather general way the effect of specific adsorption on colloid stability and then present in some detail a case study on specific adsorption of ions on hydrous oxide surface and illustrate how colloid stability is affected by the association of the oxide surfaces with H^+ and other cations.

I. Colloid Stability and Specific Adsorption

Following the assumptions of Stern, the overall standard free energy of adsorption, $\widetilde{\Delta G^0}$ is the sum of the total specific (»chemical«) adsorption energy, Φ, and the electrochemical work involved in the adsorption $zF\psi_\delta$

$$\widetilde{\Delta G^0} = -\Phi + zF\psi_\delta , \qquad (1)$$

Experimentally it is quite difficult to separate the energy of adsorption into its chemical and coulombic components. Despite this operational restriction, it is instructive to formulate a numerical example. For the adsorption of an ion on a surface of like charge, Eq. (1) indicates that the chemical contribution to the overall standard free energy of adsorption opposes the electrostatic contribution. For the adsorption of a monovalent organic ion to a surface of like charge and against a potential drop (ψ_δ) of 100 mv., the electrostatic term in Eq. (1) ($zF\psi_\delta$) is 2.3 kcal per mole. The standard chemical adsorption energy for typical sorbable monovalent organic ions is of the order of magnitude of -2 to -8 kcal per mole, thus indicating that the electrostatic contribution to adsorption easily can be smaller than the chemical contribution.

Somasundaran, Healy and Fuerstenau[1] have investigated the effects of alkyl chain length on the adsorption of alkylammonium ions on silica surfaces at pH 6.5—6.9. These authors consider that, in addition to electrostatic effects, surfactant adsortpion is influenced by the van der Waals energy of interaction between CH_2 groups on adjacent adsorbed surfactant molecules. The van der Waals cohesive energy CH_2 group is found to be approximately 1 RT (at 25^0 C RT = 595 per mole). For a 12-carbon alkylamine, the van der Waals cohesive energy is therefore of the order of 7 kcal per mole, and usually exceeds the electrostatic contribution.

Davies and Rideal[2] have reviewed the results of several investigators on the specific interaction energy arising from polarization (complex formation) and van der Waals forces for a number of surfaces. Davies and Ridael, for example, give for the specific energy of interaction on a carboxylate surface for Na^+, Mg^{2+}, Ca^{2+} and Cu^{2+} value of, respectively, $\sim -0.6 \sim -1.3$. ~ -2.6, and ~ -5.8 kcal per mole.

Polymers. — That van der Waals forces contribute significantly to the specific interaction energy is apparent from the observation that macromolecules have a strong tendency to accumulate at interfaces. For example, on an incipiently negatively charged silica surface, polystyrene sulfonate $[CH_2-CH-C_6H_4-SO_3]_n^{-n}$ is adsorbed readily, while p-toluene sulfonate ($CH_3-C_6H_4-SO_3^-$) does not adsorb from 10^{-4} M solutions. Usually the extent

of adsorption, but not necessarily its kinetics, increases with increasing molecular weight, and is affected by the number and type of functional groups in the polymer molecule. Adsorption of anionic polymers on negative surfaces is common.

Hydrolyzed Metal Ions. — The hydrolysis products of multivalent ions have a different charge than the metal ions themselves, and are adsorbed more readily at particle-water interfaces than nonhydrolyzed metal ions. This tendency to be adsorbed, even against electrostatic repulsion, is especially pronounced for polynucelar polyhydroxo species. No adequate theory for this enhanced adsorption by hydrolyzed metal ions is aivailable[3,4].

A few general features on the effect of sorption upon colloid stability may be derived from Fig. 1. The critical coagulation concentration (c. c. c.) of simple non-specifically sorbable ions Na^+, NO_3^- , Ca^{2+} , SO_4^{2-} , Al^{3+}), that is, the concentration required to destabilize a hydrophobic sol., is inversely proportional to the nth power of the charge of the counterion (n = 2 to 6) (Schulze-Hardy rule). With sorbable ions, the c. c. c. decreases with increasing ion sorbability[5]. Sorbable species that coagulate colloids at low concentrations may restabilize these dispersions at higher concentrations. When the destabilization agent and the colloid are of opposite charge, this restabilization is accompanied by a reversal of the charge of the colloidal particles (Fig. 2). Purely coulombic attraction will not permit an attraction of counter-ions
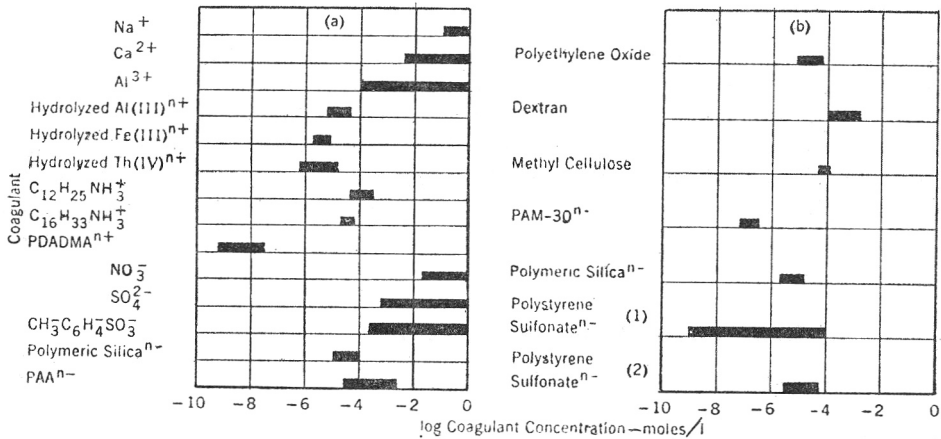
Fig. 1. Typical destabilization regions for a few representative coagulants. (From Stumm and O'Melia[4]).

(*a*) Contains coagulation regions observed when the colloid and the coagulant are of opposite charge. (*b*) Contains data obtained for the coagulation of colloids by uncharged molecules or by ions of like charge. These simplified figures are based on experimental results by various investigators that have used different experimental procedures and systems; the coagulation regions are, therefore, not always precisely comparable. The location of the coagulation regions are exemplifications, that is, they attempt to show essential features and are meaningful in a semiquantitative way only. With sorbable species, the exact location of the coagulation region on the concentration axis depends upon the concentration and surface potential of the colloids, the *p*H, the presence of other cations and anions, and the temperature. Interactions with polymers are dependent upon molecular weight and steric factors.
$PDADMA^{n+}$ = Polydiallyldimethyl-ammonium^{n+}; PAA^{n-} = Polyacrylate; PAM — 30^{n-} = Hydrolyzed (30%) phyacrylamide.
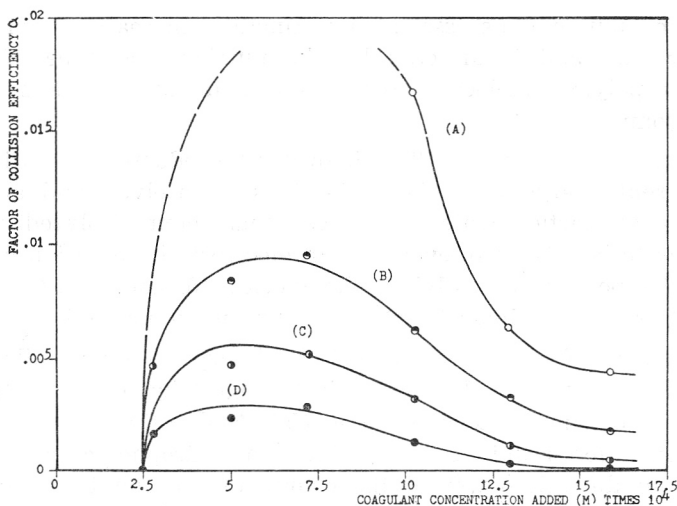
Fig. 2. Effects of pH and Al(III) dosage upon relative colloid stability of amorphorus SiO_2, expressed as collision efficiency factor, for constant surface concentration.
Diagrams such as these can be used to establish pH, Al(III), S domains, describing the limits between stable, unstable, and restabilized suspensions.

in excess of the original surface charge of the colloid. Adsorption models have been developed that depict colloid stability as a function of concentration of destabilizing species and of the surface concentration of the dispersed phase[1,6,7].

Natural and synthetic macromolecules have been used successfully as aggregating agents. Adsorption of anionic polymers on negative surfaces is common and aggregation of negatively charged colloids by polymers of like charge is possible (Fig. 1b). Hence, colloid destabilization by these materials cannot be characterized by the double layer model. La Mer and coworkers[8] and others have developed a chemical bridging theory that provides a more acceptable model for understanding the ability of polymers to destabilize colloidal suspensions.

II. The Hydrous Oxide Electrolyte Interface

The stability of hydrous oxides (Al_2O_3, FeOOH, TiO_2, SiO_2, MnO_2, etc.) is affected by electrolytes in a different way than that of hydrophobic colloids[9-12] (Fig. 3). The difference is caused primarily by the strongly structured, extensively hydrogen bonded and chemisorbed water layer immediately adjacent to the oxide surface.

In order to appreciate the surface chemical properties of hydrous oxides we will first compare from an electrochemical point of view the interface at a polarized electrode with an oxide-electrolyte interface. Then we will treat the hydrous oxide surface from a solution chemical point of view, trying to understand the association of the strongly aquated oxide surface with H^+, OH^- and cations in terms of coordination chemistry.
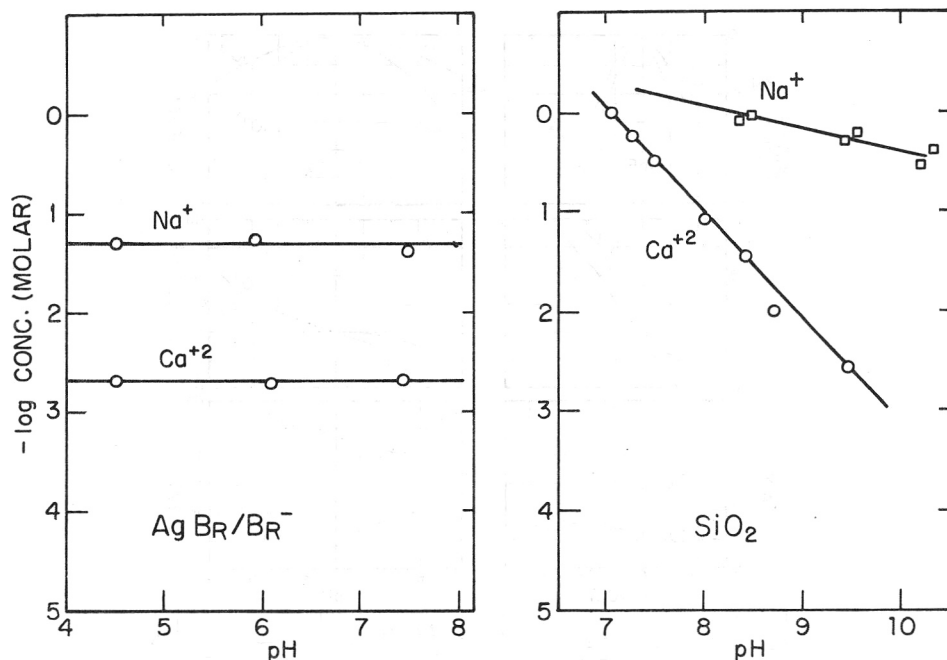
Fig. 3. Mechanisms of destabilization of hydrophobic and strongly solvated colloids. (From Data by L. H. Allen and E. Matijević.

1. The Polarized Electrode-Electrolyte and the Reversible Solid-Electrolyte Interface

Two classes of interfaces are especially suited to experimental and theoretical treatment: (1) the polarizable interface; and (2) the reversible interface. A polarizable interface is represented by a (polarizable) electrode where a potential difference across the double layer is applied *externally*, that is by applying a voltage between the electrode and a reference electrode using a potentiostat. At a reversible interface the change in electrostatic potential across the double layer results from a chemical interaction of solutes (potential determining species) with the solid. The characteristics of the two types of double layers are very similar, and they differ primarily in the manner in which the potential difference across the interface is established.[13-15]

The Polarized Interface. — A comparison of the polarized and of the reversible interface is given in Fig. 4. The representation is schematic, but in accord with available data at significant points. The data for the Hg electrode polarization curves are from Grahame[16]; the curves for the Al_2O_3 — solution interface is based on results obtained in this laboratory. With a polarizable Hg electrode, it is expedient to measure the change in interfacial tension γ with the potential of the electrode. The interfacial tension can be determined by various means, *e. g.*, by measuring the drop weight of individual drops of dropping Hg electrodes or by means of a Lippmann electro-
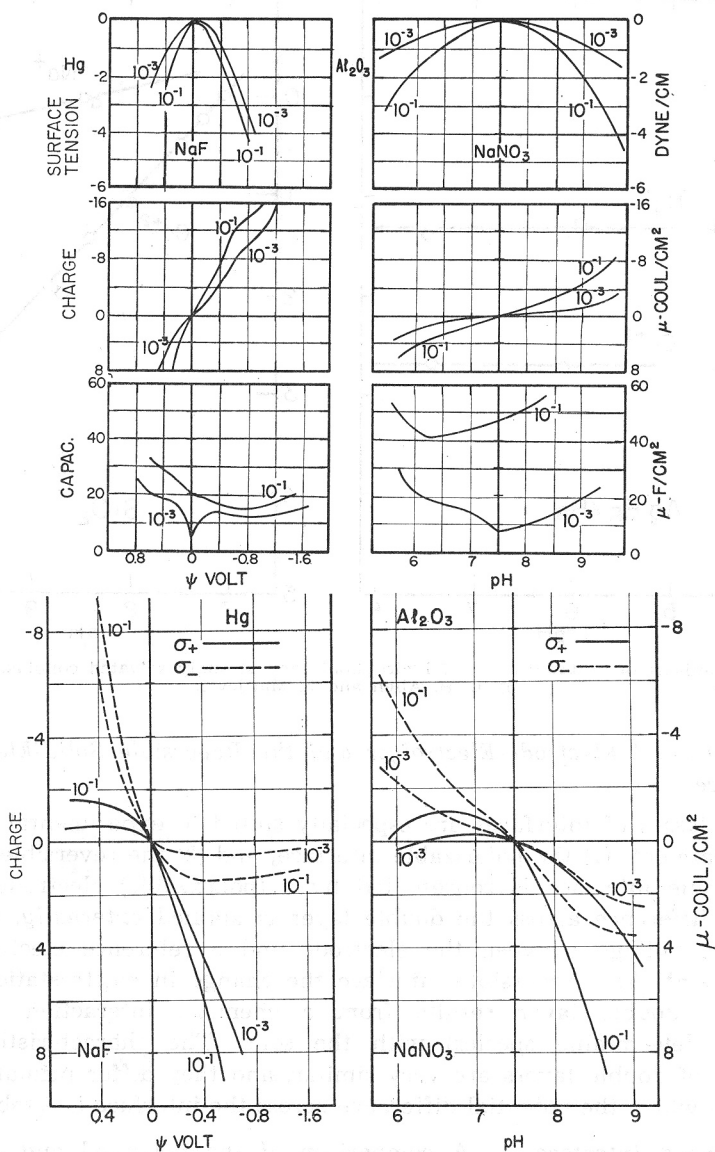
Fig. 4a and 4b. Comparison between the polarized electrode-electrolyte and the reversible oxide-electrolyte interface.

σ_+ and σ_-, the charges due to excesses at the surface of inert cations or anions, respectively, are plotted as a function of the rational potential ψ in the case of Hg and as function of pH in the case of γ—Al_2O_3.

Principally the calculated values of σ_+ and σ_- are based on measurements on the rate of change of the differential capacity of the double layer, with concentration (activity) of the electrolyte. While the curves for the Hg interface are thermodynamically self-consistent, the curves for the Al_2O_3 interface have been calculated on the assumption that $\Gamma_+ = \Gamma_- = 0$ at $\sigma_0 = 0$; this assumption has been verified approximately by analytical means.

meter. The shapes of these electro-capillary curves, depend on the nature of the solution and provide information on the equilibrium structure of the double layer and on the specific sorbability of dissolved substances. Sorbable cations or anions depress the interfacial tension especially at potentials, respectively, more negative and more positive than the electrocapillary maximum. The extent of adsorption can be predicted from the *Gibbs adsorption equation* which can be written in the form

$$\Gamma_i = - \left(\frac{\partial \gamma}{\partial \mu_i} \right) \text{T, p, all } \mu_s' \text{ other than } \mu_i \tag{4}$$

It can be shown from thermodynamics that the slope of the electrocapillary curve is equal to the charge density, σ_o, in the electrical double layer (First Lippmann Equation).

$$\left(\frac{\partial \gamma}{\partial \psi} \right)_{\text{T, p, } \mu} = - \sigma_o \tag{5}$$

At the electrocapillary maximum, the charge density σ_o is zero (point of zero change).

By definition the *differential capacity* C_d is equal to (second Lippmann Equation)

$$C_d = - \left(\frac{\partial \sigma_o}{\partial \psi} \right)_{\text{T, p, } \mu} = + \left(\frac{\partial^2 \gamma}{\partial \psi^2} \right)_{\text{T, p, } \mu} \tag{6}$$

which is the first differential of the potential dependence of charge or the second differential of the electrocapillary curve. The differential capacity can be determined directly e. g., by an a. c. method. In order to vary the electrode potential, a d. c. voltage is superimposed upon the a. c. component.

The capacity may be subdivided into a contribution within the compact layer and a capacity within the diffuse part of the double layer; these contributions being connected in series

$$\frac{\partial \psi_o}{\partial \sigma_o} = + \frac{\partial (\psi_o - \psi_2)}{\partial \sigma_o} + \frac{\partial \psi_2}{\partial \sigma_o} \tag{7}$$

as,

$$\frac{1}{C} = \frac{1}{C_{\text{comp}}} + \frac{1}{C_{\text{dif}}} \tag{8}$$

It is possible to determine C experimentally and to estimate C_{dif} with the help of the Gouy-Chapman model. At high ionic strength, ψ_2 is small and $\frac{1}{C_{\text{comp}}} \gg \frac{1}{C_{\text{dif}}}$; at low ionic strength and if ψ_2 is large, $\frac{1}{C_{\text{dif}}} > \frac{1}{C_{\text{comp}}}$. Note that the *smaller* capacity contribution mainly determines the over-all value of C. With Hg, C_{comp} is of the order of $20 \, \mu\text{Fcm}^{-2}$ when cations populate the compact layer, (negative polarized electrode), and $C_{\text{comp}} \simeq 40 \, \mu\text{F cm}^{-2}$ when anions predominate in the interface region. Apparently, at the Hg electrode anions penetrate the inner layer more efficiently than the cations.

As we have seen, the polarized electrode is readily amenable to experimental exploration. Either the electrocapillary curve or the potential

dependence of the differential capacity is determined experimentally. From either set of experimental data, individual ionic components of charge as a function of electrode charge or electrode potential can be evaluated. For specifically sorbable ions, the dependence of their surface concentration on solution concentration and electrode potential may be examined and the adsorption isotherm deduced. Hence, a rather complete and quantitative description of the distribution of ions can be made[16-18] (Fig. 4b).

The Reversible Interface. — The reversible solid-electrolyte interface provides a convenient tool to quantitatively explore the distribution of charge components at interfaces other than electrodes. However, many of the solid-solution interfaces do not approach ideality to the same extent as the polarized electrode.

Reversible interfaces can be established for solids whose surfaces are in equilibrium with potential determining species[13-15]. For inorganic oxides perhaps most accessible experimentally are data on the potential (pH)-dependent density

$$\sigma_0 = F\,(\Gamma^*_{H^+} - \Gamma^*_{OH^-}) = -F\,(\Gamma_+ - \Gamma_-) \tag{9}$$

where Γ is the surface excess (moles area^{-1}) respectively, for cations (Γ_+), anions (Γ_-), for H^+ and H^+ complexes ($\Gamma^*_{H^+}$), and for OH^- and OH^- complexes ($\Gamma^*_{OH^-}$).

$\Gamma^*_{OH} - \Gamma^*_{H^+}$ is determined from an alkalimetric titration curve. The method consists essentially of measuring the proton or hydroxide ion consumption by the solid phase, by comparing the titration curve of a suspension of the inorganic oxide with that of the medium alone (see Figs. 7 and 8)

$$\frac{C_B - C_A + [H^+] - [OH^-]}{S} = \Gamma^*_{OH^-} - \Gamma^*_{H^+} = -\frac{\sigma_0}{F} \tag{10}$$

where C_B, C_A and S are respectively concentration of strong base, strong acid and surface area concentration. The potential axis of the polarized interface can be replaced by pH provided H^+ and OH^- are potential determining ions; hence the experimentally determined σ_0 can be plotted as a function of pH. The Lippmann equations can be used as with the polarized electrodes, to obtain the differential capacity from

$$\frac{F}{RT}\left(\frac{\partial \sigma_0}{\partial pH}\right)_{\mu,\,T,\,p} = -C \tag{11}$$

and to infer the change in interfacial tension as a function of pH by integration graphically the σ_0 versus pH curve

$$\gamma = \frac{RT}{F} \int \sigma_0 \, dpH + K \tag{12}$$

where K is the integration constant.

The information provided by experimental values of σ_0 as a function of pH and of μ is thermodynamically interconnected (Gibbs Adsorption Equation) with the μ and pH dependent sorption of ionic components (Fig. 4b and Fig. 5). In Fig. 5, the evaluation of experimental data for $\gamma\text{-}Al_2O_3$ is illustrated.
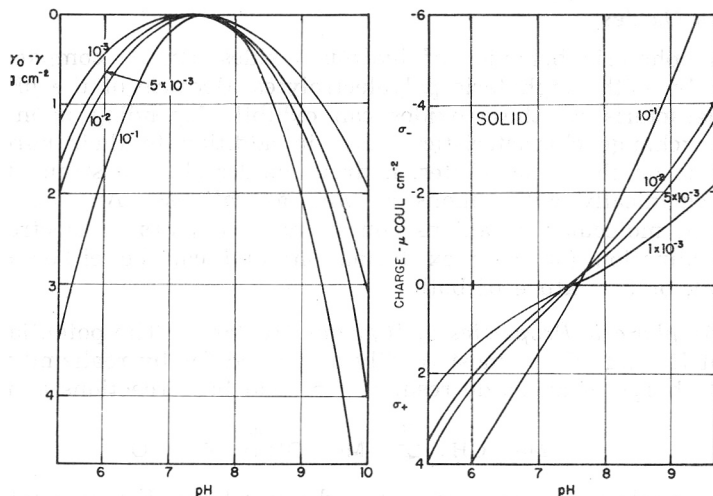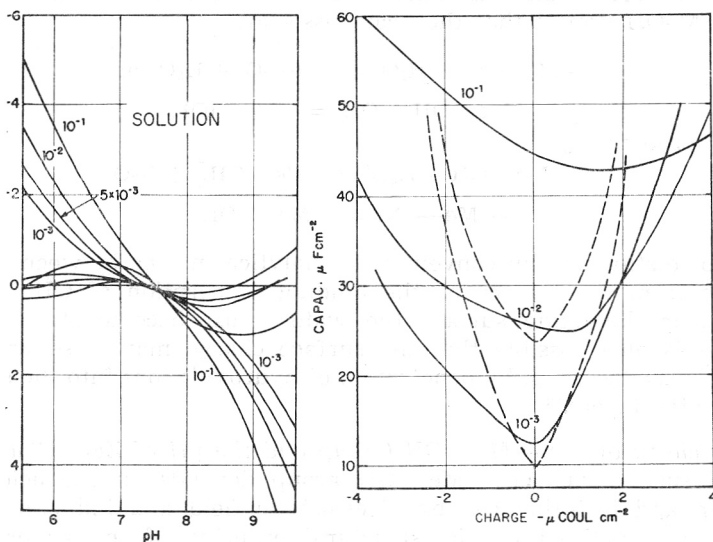
. Evaluation of double layer characteristics for γ — Al_2O_3 in $NaNO_3$ solutions.
of relative interfacial tension with pH; *b*) charge on the solid side of the double
mputed from alkalimetric titration curves; *c*) charge on the solution side of the
, $\sigma_+ = F\Gamma_+$ and $\sigma_- = F\Gamma_-$, where Γ_+ and Γ_- are the excess of cations or anions
of the double layer) present over what would be present in a column of solution
s section extending from the interface (assumed planar) into the interior of the
Grahame[16]). Thermodynamically only the shape of the curves are ascertained; as
e figure; their specific location is based on the assumption $\sigma_+ = \sigma_- = 0$ for $\sigma_0 = 0$.
res obtained for the desorption of cations at low pH and for the desorption of
h pH, respectively are probably experimental artefacts caused by the experimental
n these regions. *d*) Differential capacity as a function of σ_0. The dashed line corre-
e theoretical capacity of the diffuse part of the double layer (Gouy Chapman
low electrolyte concentrations the agreement at σ_0 between actual C and theoretical
ably good. (The small difference may be caused by an error in the specific surface
area determination).

2. *A Preliminary Approach to the Interfacial Coordination Chemistry of Hydrous Oxides*

The amphoteric behavior of hydrous oxides can be compared, at least operationally, with amphoteric polyelectrolytes. Because of the pH-dependent charge characteristics, these oxides can exhibit, depending upon pH, cation or anion exchange characteristics[19]. But in addition to their purely electrostatic effects on the ionic solutes, hydrous oxides show a strong tendency to intereact chemically with anions as well as cations[20]. Any combination of cations with molecules or anions containing free pairs of electrons may be called coordination (or complex formation) and can be either electrostatic or covalent, or a mixture of both.

The Amphoteric Properties of Hydrous Oxides. — The potential determining role of H^+ and OH^- is most readily accounted for by realizing that the pH dependent charge of an oxide results from acid base reactions at the surface:

$$—Me—OH_2^+ \underset{K_1}{\rightleftarrows} —Me—OH \underset{K_2}{\rightleftarrows} —Me—O^- \tag{13}$$
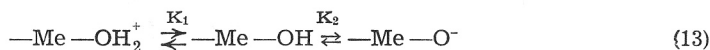
where Me stands for a metal of metaloid central ion. For an oxide, solvation (hydration) of the surface has to precede proton transfer. It is convenient to visualize the surface sites as converted upon hydration to surface hydroxo groups or MeOH groups that then can dissociate

$$—Me—OH + H_2O = —Me—O^- + H_3O^+ \text{ or} \tag{14}$$

$$—Me—OH + OH^- = —Me—(OH)_2^-$$

or accept protons

$$—Me—OH + H_3O^+ = —Me—OH_2^+ + H_2O \tag{15}$$

$$—Me—OH = —Me^+ + OH^-$$
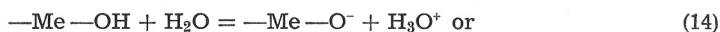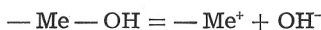
One cannot distinguish by conventional analytical means between dissociation of protons from the surface or the binding or sorption of OH^- ions to the surface. Near the oxide surface the water must become structurally well ordered; it is also possible that the surface charge may arise within a few layers of the surface, *e. g.* by penetration of hydroxide ions into the structurally ordered water layers.[13]

The Acidity of the —Me—OH Group and the pH of Zero Charge. — The acidity of such a surface —Me—OH group depends on the acidity of the central ion and is influenced by electrostatic field and induction effects of the solid and modified by the structural ordering of the water layer immediately adjacent to the solid surface. In particular, hydrogen bonding tends to facilitate proton transfer and enhance the acidity. The acidity and basicity of a surface group characterize the amphoteric properties of the hydrous oxide. The pH_{ZPC} (at the zero point of charge) is a convenient reference for expressing the pH dependent charge.

Considering the proton transfer reactions given by Equation (13) pH_{ZPC} is characterized by $[—Me—OH_2^+] = [—Me—O^-]$ and $[H^+]_{ZPC} = (K_1 K_2)^{1/2}$ or

$$pH_{ZPC} = 1/2 (pK_1 + pK_2) \tag{16}$$

where K_1 and K_2 define the acidity constants.

The Intrinsic Acidity Constant

How can mass law considerations be applied to functional groups attached to a solid surface? In Fig. 6 the acid-base behavior of a dissolved monoprotic acid such as silicic acid is compared schematically with that of a polysilicic acid and amorphous silica. With a polyvalent acid, alkalimetric and acidimetric titrations can be carried out as with mono or diprotic acids and the results can be represented similarly by ploting α (equivalent fractions of titrant added) versus pH.
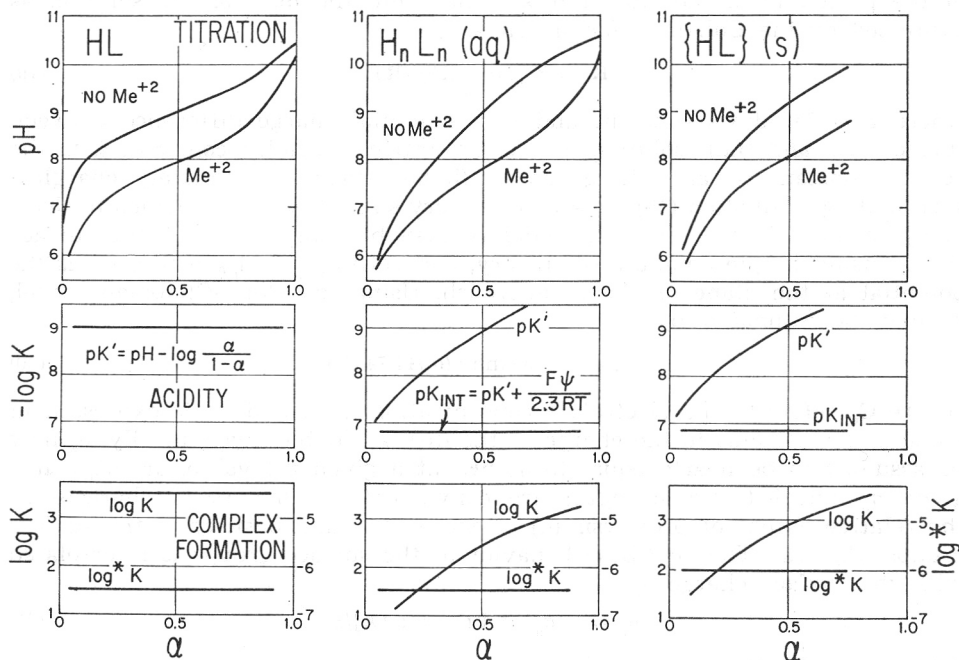
Fig. 6. Schematic representation of acid-base and complex formation behavior of monoprotic acid (e. g., H_4SiO_4), polyelectrolytic acid (e. g., polysilicic acid) and cross-linked polyacid (e. g., amorphous silica).

With increasing negative surface charge it becomes more difficult for the surface acid groups to dissociate a H^+. Similarly the tendency to associate with cations increases with increasing pH. By considering the electrostatic factor, intrinsic constants valid for acidity and complex formation for non-charged surface can be calculated.

The *ideal limiting case* assumes the following conditions: i) All acid groups are identical. (ii) The solution of dispersed polyacid is sufficiently dilute, so that interactions between dispersed different polyacids are negligible.

Define α = fraction of deprotonated acid groups; $1 - \alpha$ = fraction of protonated acid groups; hence for the polyacid ($-Si-OH)_n$:

$$\alpha = \frac{[-Si-O^-]}{[-Si-OH] + [-Si-O^-]} = \frac{[X_-]}{[X]} \qquad (17)$$

where [X] is the total sum of protolyzable groups (sometimes referred to as ion exchange capacity) in moles liters^{-1} and $[X_-] = \alpha X$.

The *microscopic acidity constant* of the —Si—OH groups is given by

$$K' = [H^+] \frac{\alpha}{1-\alpha} \tag{18}$$

Each loss of a proton reduces the charge on the polyacid and thus affects the acidity of the neighbor groups. With progressively reduced charge of the polyacid it becomes increasingly more difficult to remove a proton, thus pK' becomes larger with increasing extent of titration. The free energy of deprotonation consists of dissociation of H^+ as measured by K_{int} and of removal of the proton from the site of dissociation into the bulk of the solution as expressed by the Boltzman factor. Thus,

$$K' = K_{int} \exp (F\psi_s/RT) \tag{19}$$

where F = Faraday's constant and ψ_s = potential charge difference between surface site and bulk solution and K_{int} = intrinsic acidity constant, *i. e.*, the acidity constant of an acid group in (hypothetically) completely chargless surroundings. Equation (19) is based on a very simplified model, which neglects many factors.* In the simplest model ψ_s may be computed from the surface charge using simple double layer theory, *i. e.*, setting $\psi_s = \psi_\delta$ where ψ_δ is the potential at the plane of closest approach. Using the Gouy-Chapman model, ψ_s may be estimated by

$$\psi_\delta = 0.05 \sinh^{-1} (\sigma_s/11.74 \, C_0) \tag{20}$$

Where C_0 refers to the electrolyte concentration in M and ψ_δ is expressed in volts; σ_s corresponds to the charge of the diffuse double layer, ideally, σ_s may be assumed to be nearly equal to σ_0. pK' at a given pH value, or pK_{int} at a given σ_0 and I (ionic strength) are convenient parameters to characterize the relative extent of protolysis (α) or the acidity and basicity of the surface groups (Fig. 7a). The acid-base behavior of the surface groups is interrelated with the surface charge σ_0

$$\sigma_0 = -\sigma_{aq} = F\Gamma_- = \alpha \, [X]/S \tag{21}$$

when S is the surface area (cm^2).

Determination of the Sum of Functional Groups (Exchange Capacity)

If for hydrous oxide surfaces, the model of functional —Me OH groups is adopted, an exchange capacity ($[X] = [-Me-OH] + [-Me-O^-]$) can be defined for such surfaces. Operationally, this capacity may be determined by measuring ultimate base consumption, *i. e.*, by adding known excess of base,

---

* It is interesting to note that Equation (19) can also be derived from a consideration of Stern's treatment of the double layer. If n_c is the number of OH^- ions »sorbed« per cm^2 from a bulk concentration of mole fraction, X_{OH}, of OH^- ions, and n_s is the number of possible sorption sites in the surface, the ratio of occupied (with OH^-) to unoccupied sites may be related to the corresponding ratio in the solution as follows:

$$\frac{n_c}{n_s - n_c} = \frac{\alpha}{1-\alpha} = X_{OH} \exp [(F\psi_\delta + \Phi)/RT]$$

This can be rearranged into Eq. (19).
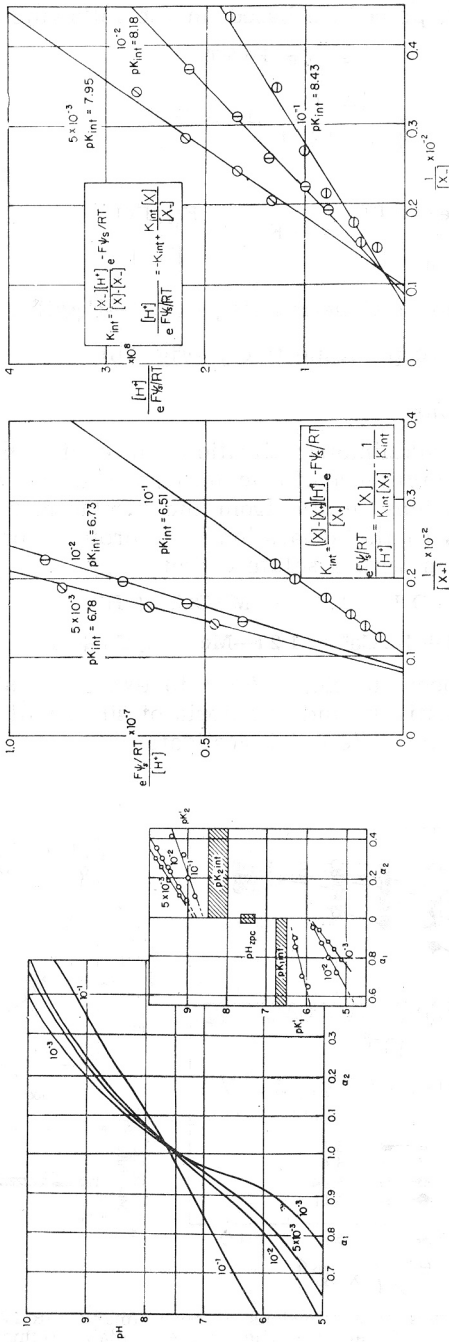
Fig. 7. The amphoteric behavior of hydrous $\gamma - Al_2O_3$

a) Alkalimetric titration curve for a suspension of $\gamma - Al_2O_3$ in presence of various concentrations of $NaNO_3$. pH of zero point of charge is 7.5 ± 0.2. From these curves, microscopic acidity constants K_1' and K_2' can be calculated; these can be corrected for an uncharged surface to intrinsic acidity constants (see insert). b) Graphical procedure to determine directly the ion exchange capacity of the oxide (*i. e.* the density of functional groups) (intersect of abscissa) and K_{int} from the slope. (For derivation see insert. The method is patterned along the lines of a Gran plot. Note the good agreement in value of [X] obtained from both steps of the titration curve.

which after separation of the solid phase, is back titrated with acid or more conveniently by a graphical procedure based on the following equations:

$$K_{int} = K'e^{-F\psi_s/RT} \tag{22}$$

$$K_{int} = \frac{[X_-]}{[X] - [X_-]} [H^+]e^{-F\psi_s/RT} \tag{23}$$

which may be written as

$$\frac{[H^+]e^{-F\psi_s/RT}}{K_{int}[X]} = -K_{int} + \frac{K_{int}[X]}{[X_-]} \tag{24}$$

Plotting $\dfrac{1}{[X_-]}$ of Equation (24) *versus* [H$^+$] exp. ($-F\psi_s/RT$) gives K_{int} and [X] from the slope and intercept, respectively (Fig. 7b).

Coordination with Metal Ions

Fig. 8 shows that the alkalimetric titration curve of a manganate (IV) suspension is affected by the presence of calcium ions. The shift in the titration curve caused by the metal ions results from the displacement of bound H$^+$ metal ions, *i. e.*, it involves (i) the separation of a proton from the covalent bond, and, (ii) the association with a solute cation, *e. g.*,

$$-Me-OH + Ca^{2+} = -Me\,OCa^+ + H^+ \tag{25}$$

or

$$-Me-OH + 1/2\,Ca^{2+} = 1/2\,(-Me-O)_2\,Ca + H^+ \tag{26}$$
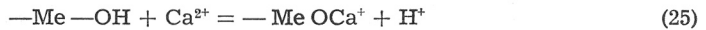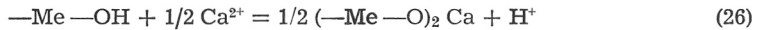
Various models have been developed[12,21-23] to express equilibria of such association reactions quantitatively and equilibria of silica with various metal ions have been determined by different investigatiors.
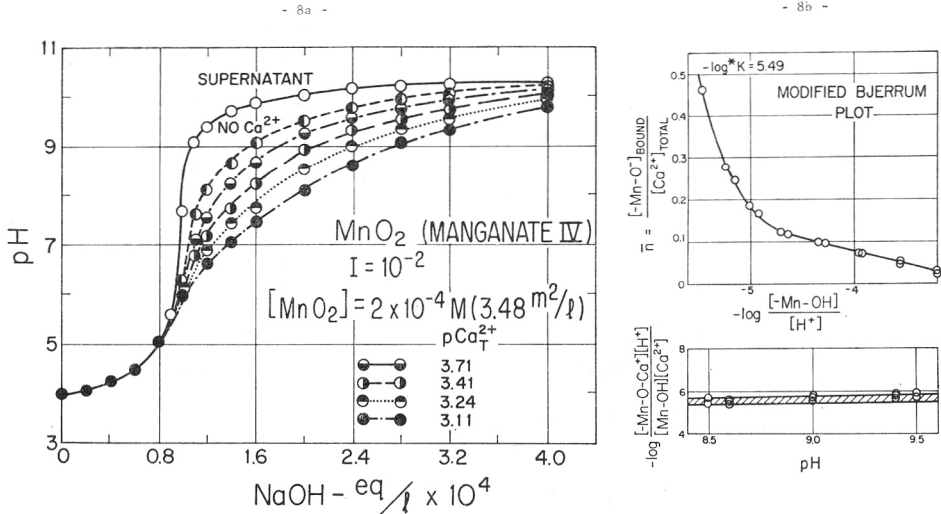
Fig. 8a. Alkalimetric titration curves of suspensions of MnO$_2$ (manganate(IV)) in presence of various concentrations of NaNO$_3$ and Ca(NO$_3$)$_2$. The samples contain originally some HNO$_3$.
Fig. 8b. Ca-Complexes of Manganate(IV). A modified Bjerrum method developed by Gregor[25] for polyelectrolytes can be applied to compute stability constants. b$_1$ values calculated directly with experimentally determined values of ꞌ[—Me—OCa$^+$], [H$^+$], [—Mn—OH] and [Ca^{2+}]. Shaded area shows limits of values for b$_1$ determined by the modified Bjerrum method.

Association of Counterions

From the theories of Debye and Huckel, it is known that association (ion pair formation) between simple monovalent cations and anions is slight for dilute salt solutions. Going to multivalent ions the tendency to ion pair formation increases in accordance with Bjerrum's theory. As more charged groups are fixed together, the overall degree of association between ions of opposite charge increases.

Ca^{2+} is able to reverse the electrophoretic mobility of a manganate (IV) suspension at $pH = 7$. Ionic species sorbed in response to coulombic attraction alone, obviously, cannot sorb in amount larger than those equivalent to the original surface charge. However, any ion that enters the compact layer can modify the double layer structure in such a way that the charge of the diffuse layer may become reversed. The thermodynamic model which has been used, defines σ_0 as the surface charge due to »specific sorption« of potential determining OH^- or H^+ ions; this model must now be amended so that a layer of specifically adsorbed (but not potential determining) cations can be placed between the surface charge and the diffuse layer. Thus, a negatively charged surface might be balanced by the positive charge of specifically adsorbed cations and the negative charge of the diffuse double layer; the latter being reflected by a positive electrophoretic mobility. The charge balance in the presence of $NaNO_3$ and $Ca(NO_3)_2$ is given by:

$$\sigma_0 = F\,(\Gamma_H^+ - \Gamma_{OH-}) = F\,(\Gamma_{NO_3^-} - \Gamma_{Na^+} - 2\,\Gamma_{Ca^{2+}}) \tag{27}$$

A similar reversal of charge by bivalent nonhydrolyzed ions has been demonstrated[10,24]. Recently, Healy et al.[10] showed that the charge on quartz at $pH = 7$ can be reversed by 10^{-4} M Ca^{2+}.

Evaluation of the Stability Constant from Alkalimetric Titration Curves

Fig. 8 shows titration curves in the presence of various $[Ca^{2+}]$ obtained at constant ionic strength. At a given pH we assume equivalent donor sites:

$$\alpha = \frac{[-Mn-O^-]}{[-Mn\,O^-] + [-Mn-OH]} = \frac{[-Mn-O^-]}{[X]} \tag{28}$$

if $[Ca^{2+}] = 0$, the titration curve is characterized by:

$$C_B = \alpha\,[X] + [OH^-] - [H^+] \tag{29}$$

where C_B is the concentration of strong base (NaOH) in the solution.

If $[Ca^{2+}] > 0$, the charge balance for the titration curve can be formulated as

$$C_B' = \alpha\,[X] + (1-\alpha)\,[-Mn-OCa^+] + [OH^-] - [H^+] \tag{30}$$

If one assumes the reaction

$$Ca^{2+} + -Mn-O^- = -Mn-OCa^+ \tag{31}$$

the extend of Ca^{2+} coordination is related to the shift in the titration curve (see Fig. 8); at constant pH, $C_B' - C_B = \Delta C_B$ is related to the extent of association of Ca^{2+} to the $-Mn-O^-$ groups:

$$\frac{\Delta C_B}{1-\alpha} = [-Mn-OCa^+] \tag{32}$$

This relationship can be shown to apply also to a more general case where any number of complexes of Ca^{2+} and $-Mn-O^-$ are formed:

$$\frac{\Delta C_B}{1-\alpha} = \Sigma\, i\, [(-Mn-O^-)_i\, Ca^{2-i}] \tag{33}$$

One may define the following microscopic stability constants:

$$K_1 = \frac{[-Mn-OCa^+]}{[-Mn-O^-]\,[Ca^{2+}]} \tag{34}$$

and

$$b_1 = \frac{[-Mn\;OCa^+]\,[H^+]}{[-Mn\;OH]\,[Ca^{2+}]} \tag{35}$$

The ligand number or formation function $\bar{n}$ measures the number of ligands (in this case, $-Mn-O^-$) found to Ca^{2+} ion, totally present in solution

$$\bar{n} = \frac{\Sigma i\,[(-Mn-O^-)_i\, Ca^{2-i}]}{[Ca_T^{2+}]} = \frac{\Delta C_B}{(1-\alpha)\,[Ca_T^{2+}]} \tag{36}$$

The formation curve — a plot of this ligand number versus the ligand concentration — illustrates the coordination tendency of the ligand and shows under what conditions of free ligand concentrations, multidentate complexes are being formed.

As Fig. 8b documents for manganate (IV), under conditions of our experiments only values of $\bar{n} \leqq 0.5$ were obtained, thus suggesting that only monodentate associations ($-Mn-OCa^+$) are being formed.

It must be recognized that it is not possible to obtain expressions for the stability constants which are both thermodynamically meaningful and conveniently applicable to treat readily accessible experimental data.

A procedure which so far has been found most expedient for extracting stoichiometric stability quotients from experimental data is based on Gregor's[25] method for determining stability constants for polyelectrolytes. This method is a modified Bjerrum method employing Equation (35). As Gregor has shown for polyelectrolytes stability constants (b_i values) obtained from a formation curve are less dependent on charge than K_1 values. If $\bar{n}$ is plotted as a function or $\log\,([H^+]/[-Mn-OH])$, b_1, is obtained at $\bar{n} = 0.5$ from

$$b_1 = \left(\frac{[H^+]}{[-Mn-OH]}\right)_{\bar{n}=0.5} \tag{37}$$

As Fig. 8b shows $-\log b_1$ values, obtained experimentally with solutions of two different [X], are reasonably constant and pH independent. Hence, for any pH value — and at given I $(NaNO_3)$ — the extent of association of MnO_2 with Ca^{2+} can be predicted by Equation (35). This Equation can also be converted into an equation of the Langmuir form

$$[Mn-OCa^+] = \frac{[X]\,[Ca^{2+}]}{[H^+]/b_1\,(1-\alpha)\,+\,[Ca^{2+}]} \tag{38}$$

where the first term in the denominator is related to the free energy of the association reaction. Fig. 9 illustrates the application of Equation (38) to complex formation of Ca^{2+} by $\gamma - Al_2O_3$. In this case Equation (38) has been rearranged into the form

$$\frac{1}{[Al-OCa^+]} = \frac{1}{[X]} + \frac{[H^+]}{b_1 (1-\alpha) [X] [Ca^{2+}]} \tag{39}$$

which can be plotted from data readily accessible experimentally. The left hand side of the Equation (39) is equivalent to $(1-\alpha)/\Delta C_B$ (cf. Equation (33). $[Ca^{2+}]$ is obtained by an iterative procedure. Although not representing a thermodynamically rigorous formulation for stability, because the concentra-
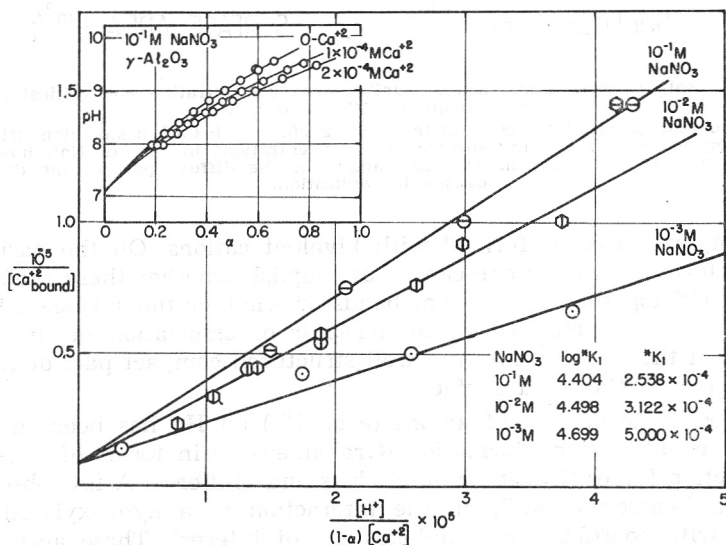
Fig. 9. Methods used in evaluating the stability of surface complexes. Ca-Complexes of $\gamma-Al_2O_3$. Graphical evaluation according to Equation (39).

tion terms were not corrected for the electrostatic term $e^{-F\psi_s/RT}$, Equation (34) is of practical and predictive value. It may, for example, be used to predict adsorption isotherms or estimate colloid stability of hydrous oxides. Fig. 10 shows that in the pH range studied there exists a stoichiometric relationship between c.c.c. of Ca^{2+} and the concentration of the MnO_2 colloid. If Ca^{2+} caused simply a compaction of the diffuse part of the double layer the c.c.c. of Ca^{2+} would be virtually independent of colloid concentration. Because of the specific chemical interaction, the c.c.c. of Ca^{2+} depends on the concentration of the solid surface[4]. Destabilization by Na^+ on the other hand, is characterized by a c.c.c. independent of the concentration of the dispersed phase, indicative that little of the Na^+ becomes specifically sorbed on the colloid surface. Equations (34) or (35) permitted satisfactorily the prediction of c.c.c. values of Ca^{2+} for various pH values and surface concentration of MnO_2[30].

The results obtained on the pH-dependent association of »δ-MnO_2« [Manganate (IV)] and of $\gamma - Al_2O_3$ with Ca^{2+}, illustrate that moderately strong
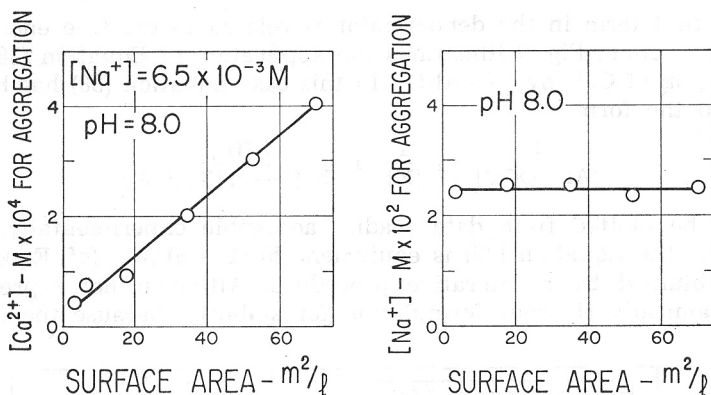
Fig. 10. Relationship between MnO_2 colloid surface area concentration and critical coagulation concentration of Ca^{2+} and Na^+.
Because of the specific interaction of the oxide surface with Ca^{2+}, a stoichiometric relationship exists between c. c. c. and the surface area concentration; in case of Na^+, however, this interaction is weaker, so that primarily compaction of the diffuse part of the double layer causes destabilization.

surface complexes can be formed with bivalent cations. On the basis of the available information alone one cannot distinguish whether these surface complexes are held together by covalent bonds or whether the surface interaction is more readily characterized by an ion-pair of association or by a simple penetration of the Ca^{2+} ion into the well structured compact part of the water layer, adjacent to the solid surface.

The specific adsorption of anions (e. g., Cl⁻) on Hg has been interpreted in terms of covalent bond formation (Grahame[16]) or in terms of purely physical interaction forces (Devanathan, Bockris and Müller[26]). A few observations by Burwell, Pearson et al.[27], on the interaction of a hydroxylated surface (silica gel) with coordination complexes are of interest. These authors show that labile coordination complexes (such as ammino nickel complexes) adsorbed on silica gel exhibit normal reactivities; i. e., such complexes readily interchange ligands such as water and ammonia. On the other hand, inert complexes that contained an H_2O ligand (e. g. [trans-Co(III) en₂ Cl₂ aq]⁺) react with surface silanol groups to bind the silanolato group into the coordination sphere. While labile complexes are rapidly extracted with HCl, bound inert complexes cannot be removed readily from the silica by HCl.

Polarity of the Solid. — The polarity of the solid must also effect the extent of the ionic interaction at the surface. This is also apparent from the observation that solids of the same chemical surface composition such as »δ-MnO_2« [Manganate (IV)] and β-MnO_2 (Pyrolusite) can show an opposite affinity sequence for Na^+ and Cs^+ ions. Cs^+ is preferred over Na^+ by manganate (IV) (»δ-MnO_2«) while Na^+ is sorbed preferably over Cs^+ pyrolusite (β-MnO_2). Such an effect must largely be accounted for by the influence which electrostatic crystal field strength has on the structure of the adjacent water layer and on the coulombic interaction of surface ionic groups with cations[13,29].

Fig. 11 shows C values (differential capacity) as a function of charge density, σ_0, for various solids. A comparison shows that in dilute solutions
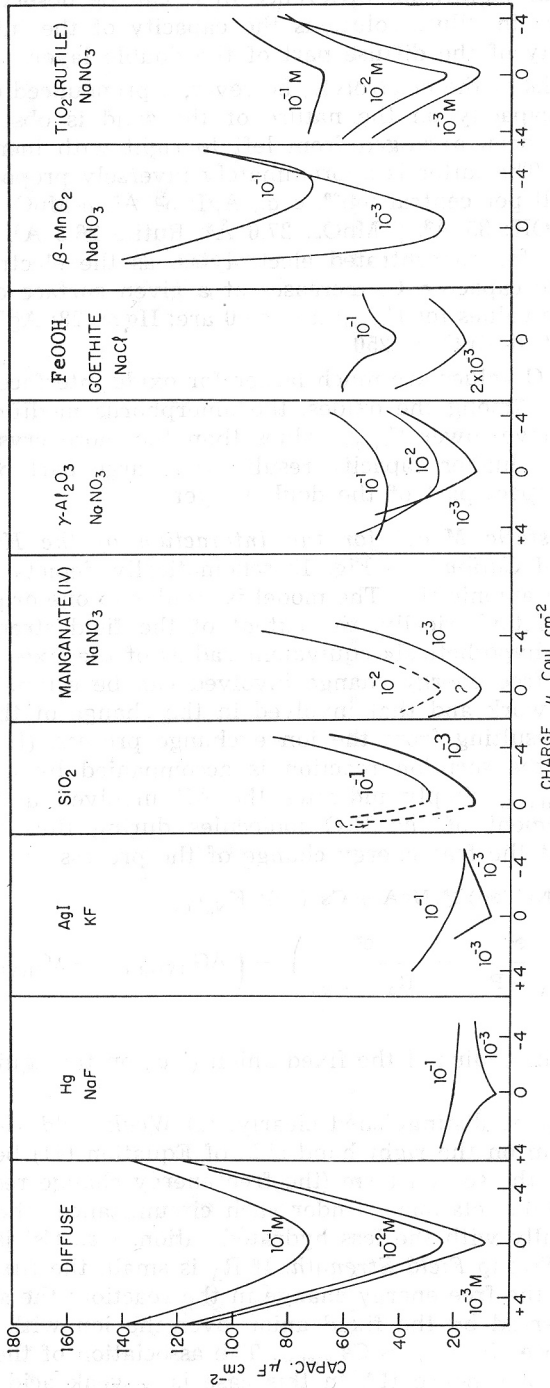
Fig. 11. Differential capacity values plotted as a function of charge density σ_0 for various interfaces.

Theoretical values for diffuse double layer have been computed according to the Gouy Chapman theory of single flat double layer. C values plotted for Hg, AgI and TiO$_2$ are from Grahame[16], Lyklema[15] and DeBruyn[18], respectively. C values plotted for oxides have been obtained from alkalimetric and acidimetric titration curves carried out with dispersions of oxides in the appropriate electrolyte solutions. Determination of specific surface area were made by BET methodology.

For an uncharged surface the differential capacity of dilute solutions ($I = 10^{-3}$ M) is independent of type of surface because C is controlled predominantly by C_{dif} (the capacity in the diffuse part of the double layer.) In more concentrated solutions C becomes controlled by C_{comp} (capacity of the compact layer) C_{comp} depends critically on the type of double layer. For hydrous oxides C_{comp} is significantly larger than for Hg and AgI. With increased polarity of the surface (from left to right) C_{comp} increases thus indicating an increase in penetration by ions into the compact part of the double layer the higher the electrostatic field strength of the solid; concomittantly the extent of electrostriction of chemisorbed water adjoining the solid surface is presumably increased.

(10^{-3} M of 1:1 electrolyte) no significant difference in C can be observed for the different solids, that is, in dilute solutions the capacity of the interface is controlled by the capacity of the diffuse part of the double layer.

At higher ionic strengths of the electrolyte, however, a pronounced dependence of the differential capacity on the nature of the solid is observed[13]. In Fig. 11, the solids have been arranged from left to right with increasing electrostatic field strength. The latter is approximately inversely proportional to the value of the unit cell per central ion[29], e. g., AgI: 54 Å^3, δ-MnO$_2$ [Manganate (IV)]: 44 Å^3, α-FeOOH: 35 Å^3, β-MnO$_2$: 27.6 Å^3, Rutile 26.2 Å^3. It can be seen from Fig. 11, that for concentrated electrolytes, as the electrostatic field strength increases, the capacity, C, increases at a given surface charge. Representative approximate values for C_{comp} at $\sigma_0 \approx 0$ are: Hg $\approx$ 28; AgI $\approx$ 30; δ-MnO$_2 \approx$ 40, γ-Al$_2$O$_3 \approx$ 90, β-MnO$_2 \approx$ 250.

It is apparent that the C values are much larger for oxide interfaces than for Hg and AgI interfaces. Among the oxides, the amorphorus modifications (amorph. SiO$_2$, »δ-MnO«) have lower C_{comp} values than the more crystalline and more popular solids. A higher capacity results to a large part because ions penetrate into the compact part of the double layer.

A Semiquatitative Electrostatic Model for the Interaction of the Hydrous Oxide Surface with H$^+$ and Cations. — Fig. 12 schematically depicts an ion exchange process at a fixed anionic site. The model is similar to one originally proposed by Eisenman[28]. Metaphorically, the extent of the field strength is expressed in terms of the »hypothetical« equivalent radius of the fixed anion. As Fig. 12 illustrates, the free energy change involved can be estimated by considering the coulombic work and that involved in the change of the H$_2$O — coordinative relations resulting from the ion exchange process. (It is not necessary to assume that the sorption reaction is accompanied by a dehydration of the cation. ΔG_{HYDR} simply indicates the ΔG involved in partial displacement or rearrangement of the H$_2$O molecules during the sorption process). It is apparent that the free energy change of the process

$$CsA + Na^+ (aq) \rightleftarrows NaA + Cs^+ (aq); \quad K_{Na^+/Cs} \tag{40}$$
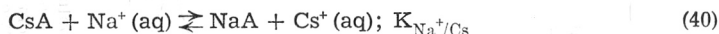
$$G = -RT \ln K_{Na^+/Cs^+} = \left(\frac{e^2}{R_A + R_{Cs}} - \frac{e^2}{R_A + R_{Na}} \right) - \left(\Delta G_{HYDR(Cs)} - \Delta G_{HYDR(Na)} \right) \tag{41}$$

is critically dependent on the radius of the fixed anion (*i. e.*, on the equivalent field strength).

Two extreme cases can be distinguished clearly: (1) *Weak field strength.* If R_A is large, the first term on the right hand side of Equation (41) becomes negligible in comparison to the second term (the free energy change resulting from change in the hydration relations). Under such circumstances the fixed anion associates preferentially with the less hydrated cation, *i. e.*, Cs$^+$ is more strongly sorbed than Na$^+$. *Strong Field Strength.* If R_A is small, the first term in Equation (41) dominates the free energy change in the reaction; the smaller (non-hydrated) ion is preferred by the fixed anion over the ion with larger radius. In this case, therefore Na$^+_{sorbed}$ > Cs$^+_{sorbed}$. The association of the fixed anion with H$^+$ is a strong one, hence HA in this case is a weak acid cation exchanger, such as resins with COOH groups, soda glass and strongly polarized

$$\Delta G' = \frac{e^2}{R_A + R_2} - \Delta G_{Hydr(2)}$$

Bulk Solution
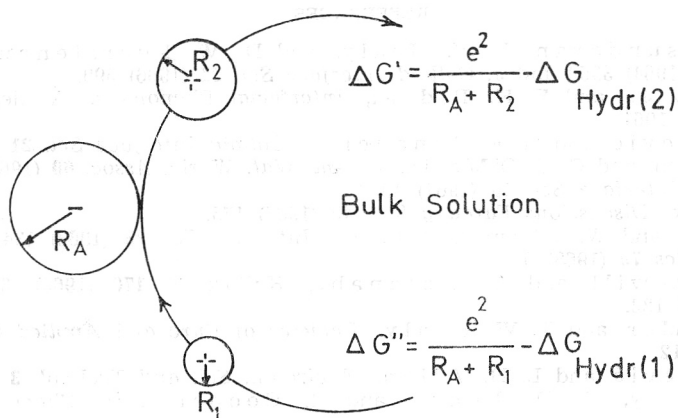
$$\Delta G'' = \frac{e^2}{R_A + R_1} - \Delta G_{Hydr(1)}$$

$$\Delta G = -RT \ln K_{1/2} = \left(\frac{e^2}{R_A + R_2} - \frac{e^2}{R_A + R_1} \right) - (\Delta G_{Hydr(2)} - \Delta G_{Hydr(1)})$$

Exchange Reaction: $CsA + Na^+ (aq) \rightleftarrows NaA + Cs^+ (aq)$; $K_{Na/Cs}$
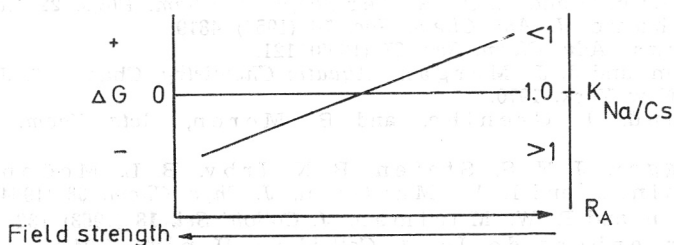
$H^+ > Na^+ > Cs^+$	$Cs^+ > Na^+ > H^+$
HA = Weak Acid	HA = Strong Acid
β-MnO_2	»δ-MnO_2«
SiO^-	Si—O—Al
$RCOO^-$	RSO_3
H^+ — Selective	Cation Selective
Strong Structured H_2O	Weak Structured H_2O

Fig. 12. Ion exchange at a fixed anionic site. The free energy change involved can be estimated by considering the coulombic work and that involved in the change of the state of hydration. The model explains why at a high field strength the small ion is preferred over the larger one.

surfaces such as β-MnO_2, TiO_2 (Rutile). According to this model increased polarity of the solid decreases the acid strength to the —Mn—OH groups. Among oxides with tetravalent central ion, the most polar solid should have the highest pH_{ZPC}. This is in accord with observations made in the present study and those of Healy, Herring ad Fuerstenau[29] who observed a progressive increase in pH_{ZPC} for δ-MnO_2, α-MnO_2, γ-MnO_2' and β-MnO_2, respectively. Similarly TiO_2 (Rutile) has a relatively high pH_{ZPC} (7.5)[13].

REFERENCES

1. P. Somasundaran, I. W. Healy, and D. W. Fuerstenau, *J. Phys. Chem.* **68** (1964) 3562 and *J. Colloid Interface Sci.* **22** (1966) 599.
2. J. T. Davies and E. K. Rideal, *Interfacial Phenomena,* Academic Press, New York, 1961.
3. E. Matijević and G. E. Janauer, *J. Colloid Interface Sci.* **21** (1966) 197.
4. W. Stumm and C. R. O'Melia, *J. Am. Wat. Works Assoc.* **60** (1968) 522 and *J. Colloid Interface Sci.* **59** (1967) 1353.
5. B. Težak, *Discussions Faraday Soc.* **42** (1967) 175.
6. H. Hahn and W. Stumm, *J. Colloid Interface Sci.* **28** (1968) 134 and *Adv. Chem. Series* **79** (1968) 91.
7. R. J. Ottewill and A. Watanabe, *Kallord F.* **170** (1960), 38, **171** 33; **173** 7; **173** 122.
8. V. K. LaMer and T. W. Healy, *Reviews of Pure and Applied Chemistry,* **13** (1963) 112
9. E. Matijević and L. H. Allen, *Environm. Sci. and Technol.* **3** (1969) 264.
10. T. W. Healy, R. D. James, and R. Cooper, *Adv. Chem. Series* **79** (1968) 62.
11. D. J. Murray, T. W. Healy, and D. W. Fuerstenau, *Adv. Chem. Series* **79** (1968) 74.
12. J. J. Morgan and W. Stumm, *J. Coll. Sci.* **19** (1964) 347.
13. Y. G. Berubé and P. L. DeBruyn, *J. Colloid Interface Sci.* **27** (1968) 305.
14. J. Lyklema and J. Overbeek, *J. Colloid Sci.* **16** (1961) 501.
15. J. Lyklema and J. Overbeek, *Trans. Faraday Soc.* **59** (1963) 418 and *Discussions Faraday Soc.* **43** (1966).
16. D. C. Grahame, *Chem. Rev.* **41** (1947) 441.
17. D. C. Grahame, and B. A. Soderberg, *J. Chem. Phys.* **22** No. 3 (1954).
18. D. C. Grahame, *J. Am. Chem. Soc.* **76** (1954) 4819.
19. G. A. Parks, *Adv. Chem. Ser.* **67** (1968) 121.
20. W. Stumm and J. J. Morgan, *Aquatic Chemistry,* Chapter 9, John Wiley and Sons, New York, 1970.
21. S. Ahrland, I. Grenthe, and B. Moren, *Acta Chem. Scand.* **14** (1968) 1059.
22. D. L. Dugger, J. H. S. Staten, B. N. Irby, B. L. McConnell, W. W. Cummings, and R. W. Maatman, *J. Phys. Chem.* **68** (1964) 757.
23. J. Stanton and R. W. Maatman, *J. Colloid Sci.* **18** (1963) 132.
24. H. G. Burgenberg de Jong, *Colloid Sci.* II, p. 239 (1949).
25. H. P. Gregor, L. B. Luttinger, and E. M. Loebl, *J. Phys. Chem.* **59** (1955) 34.
26. M. A. V. Devanathan, O. M. Bockris, and K. Müller, *Proc. Roy. Soc.* London, **A 274** (1963) 55.
27. R. L. Burwell, R. G. Pearson, G. L. Haller, P. B. Tjok, and S. P. Crock, *Inorganic Chem.* **4** (1965) 1123.
28. G. Eisenman in *Glass Electrodes for Hydrogen and other Cations,* M. Dekker, New York, 1967.
29. T. W. Healy, A. P. Herring, and O. W. Fuerstenau, *J. Colloid Interface Sci.* **21** (1966) 435.
30. S. R. Jenkins, *The Colloid Chemistry of Hydrous MnO_2 as Related to Manganese Removal,* Thesis (unpublished) Harvard University, (1960).

IZVOD

Specifične kemijske interakcije koje utječu na stabilnost disperznih sistema

W. Stumm, C. P. Huang i S. R. Jenkins

Poznato je da specije koje se adsorbiraju, utječu na stabilnost koloida kod mnogo nižih koncentracija nego ioni koji se ne adsorbiraju. Model dvosloja po Derjagin-Landau-Verwey-Overbeeku zanemaruje dominantnu ulogu kemijskih sila u adsorpciji. Zbog toga je taj model ograničen u primjeni na liofilne koloide i jednostavne elektrolite.

Uspoređivanjem diferencijalnog kapaciteta dvosloja na granici faza oksid-elektrolit s onim za Hg ili AgJ, utvrđeno je da je taj kapacitet znatno veći za hidrofilnu, jako hidratiziranu, površinu oksida, nego za hidrofobnu površinu Hg ili AgJ. Razlogom tome je ponajviše jako strukturirani i čvrstim hidrogenskim vezama vezan, kemisorbirani sloj vode neposredno uz čvrstu površinu oksida. Ioni iz elektrolita imaju tendenciju penetracije (specifična adsorpcija) u kompaktni dio dvosloja uz površinu oksida, i time utječu na kemijska svojstva površine znatno preko mjere, koju se može očekivati kompresijom difuznog dijela dvosloja.

Stupanj asocijacije oksidne površine s H⁺ ionom i drugim kationima može se karakterizirati, kao i kod polielektrolita, kiselošću i konstantama stabilnosti. Ako ih se korigira na vrijednost za hipotetičku površinu bez naboja, te konstante mogu biti izražene kao intrinzične. Potrebni su samo vrlo jednostavni elektrostatički modeli da bi se objasnila asocijacija površine s kationima, te protumačili efekti poput onih Ca^{2+} na hidroksidne koloide, ili pojave precipitacije MnO_2 čestica na pijesku. Mjera za specifičnu adsorpciju odražava se i na kritičnu koagulacionu koncentraciju. Kada su specifički adsorbirana specija i koloid suprotnog naboja, adsorbirana specija smanjuje površinski naboj koloida. U nekim slučajevima vrsta, koja uzrokuje destabilizaciju, može također i promijeniti naboj koloida i prouzrokovati ponovnu stabilizaciju.

Specifične interakcije kationa, ovdje opisane, osnova su za tumačenje sličnih specifičnih ionskih procesa, kao što su ponašanje ionski-selektivnih staklenih ili membranskih elektroda, selektivni permeabilitet ćelijskih membrana, te mehanizam stvaranja potencijala u živim ćelijama.

LABORATORY OF APPLIED CHEMISTRY
        HARVARD UNIVERSITY
        CAMBRIDGE, MASS. USA